J. Chem. Sci. Vol. 127, No. 10, October 2015, pp. 1785–1794.
DOI 10.1007/s12039-015-0940-9

A first-principles study of chlorine adsorption characteristics on α-Cr_2O_3 nanostructures

V NAGARAJAN and R CHANDIRAMOULI*
School of Electrical & Electronics Engineering, SASTRA University, Tirumalaisamudram, Thanjavur 613 401, India
e-mail: rcmoulii@gmail.com

MS received 3 April 2015; revised 15 July 2015; accepted 15 July 2015

Abstract. The structural stability, electronic and adsorption properties of chlorine on pristine, Zn, W and N-substituted α-Cr_2O_3 nanostructures are successfully optimized and simulated with the help of density functional theory utilizing B3LYP/ LanL2DZ basis set. The structural stability of α-Cr_2O_3 nanostructures are discussed in terms of formation energy. The electronic properties of pristine, Zn, W and N-substituted α-Cr_2O_3 nanostructures are described with HOMO-LUMO gap, ionization potential and electron affinity. Dipole moment and point symmetry group of pristine, Zn, W and N-substituted α-Cr_2O_3 nanostructures are reported. The adsorption characteristics of Cl_2 on α-Cr_2O_3 materials are investigated and the prominent adsorption sites of Cl_2 on α-Cr_2O_3 nanostructures are identified. The important parameters such as adsorbed energy, energy gap, average energy gap variation and Mulliken population analysis are used to find the favourable adsorption site of Cl_2 on α-Cr_2O_3 base material. The substitution of impurities such as Zn, W and N in α-Cr_2O_3 nanostructures enhances the Cl_2 adsorption characteristics in the mixed gas environment.

Keywords. Chromium oxide; nanostructures; adsorption; Mulliken population; adsorbed energy.

1. Introduction

In recent years, research is focused on metal oxide semiconductor (MOX) based chemiresistive gas sensors.[1] The surface reactivity of MOX nanostructures depends on the binding species, which is influenced by change in electron affinity and surface potential variations of adsorbent. The transfer of electrons between the adsorbent and base material leads to the change in the resistance of the thin film. Moreover, the exchange of charge carriers can be measured using electrical resistance measurement, whereas the surface potential variation can be sensed by change in the work function. The combined variation of resistance and work function provides the estimation of surface reactivity of gas on the base material. Besides the synthesis of MOX with control on size, shape, surface-to-volume ratio enhances the sensitivity of base material towards target gas.[2,3] The main requirement of sensitivity, selectivity, response towards target gas is important criterion in chemiresistive based MOX gas sensors. Generally, n-type transition metal oxide semiconductors, such as, WO_3, SnO_2, ZnO and In_2O_3 have been used in commercial applications[4,5] owing to the fact that it is extensively studied for their gas sensing mechanism. On the other hand, there is not much work reported in p-type semiconductor. One among the p-type semiconductor is chromium oxide (Cr_2O_3). Cr_2O_3 finds its potential application in optical coating, infrared sensors and catalytic reactions. The experimental energy band gap value for Cr_2O_3 is $\sim$3.4 eV.[6–9] However, pristine Cr_2O_3 was reported with poor gas sensitivity. The gas sensing properties of the materials can be enhanced with surface activation or substitution of impurities into pristine Cr_2O_3.

Chlorine (Cl_2) is one of the hazardous gases, which is an exhaust gas from industries related with textiles, plastics, pharmaceuticals, household cleaning products, agrochemicals and water purification, etc. According to Occupational Safety and Health Administration (OSHA) standard the permissible exposure limit (PEL) for chlorine is 1 part per million (ppm) for a period of 15 minutes. Cl_2 gas is harmful to life, beyond the threshold limit; Cl_2 produces skin irritation, sensory irritation, suffocation, bronchospasm, etc.[10] This necessitated the detection of toxic Cl_2. Chromium oxide exhibits in different phases namely rutile CrO_2, corundum Cr_2O_3, three-dimensional framework Cr_5O_{12}, etc. Maldonado *et al.*[11] studied the structure, electronic and magnetic properties of Ca-doped chromium oxide using density functional theory method. Blacklocks *et al.*[12] reported XAS study of defect structure in Ti-doped α-Cr_2O_3. Density functional theory (DFT) is one of the most

*For correspondence

prominent methods to investigate the adsorption properties of compounds and gases.[13] In this regard, literature survey was conducted using CrossRef metadata search and it is revealed that there are not much works reported based on DFT methods to investigate the adsorption properties of Cl_2 on α-Cr_2O_3 nanostructures. The motivation behind the present work is to enhance Cl_2 adsorption characteristics on α-Cr_2O_3 nanostructures with incorporation of suitable impurities such as Zn, W and N. The novel aspect of this work is to study the adsorption characteristics of Cl_2 on different sites of α-Cr_2O_3 nanostructures with the substitution of Zn, W and N and the results are reported.

2. Computational Methods

The pristine, Zn, W and N-substituted α-Cr_2O_3 nanostructures are optimized successfully using Gaussian 09 package.[14] The adsorption characteristics of Cl_2 gas on α-Cr_2O_3 base material is also investigated with Gaussian package. In the present work, DFT method is used along with Becke's three-parameter hybrid functional in combination with Lee-Yang-Parr correlation functional (B3LYP) with the help of LanL2DZ basis set.[15] The choice of suitable basis set is one of the important criterions for studying α-Cr_2O_3 nanostructures. Since the atomic numbers of chromium and oxygen are twenty four and eight, respectively, LanL2DZ basis set is a good choice among other basis sets. It gives an optimum output with pseudo potential approximation.[16,17] The HOMO-LUMO gap and density of states spectrum (DOS) of α-Cr_2O_3 nanostructures is recorded using Gauss Sum 3.0 package.[18] The energy convergence is attained in the range of 10^{-5} eV while optimizing α-Cr_2O_3 nanostructures.

3. Results and Discussion

The main objective of this work is to study the ionization potential (IP), formation energy, HOMO-LUMO gap, electron affinity (EA), dipole moment and the adsorption characteristics of Cl_2 gas on α-Cr_2O_3 base material with the substitution of impurities, such as, Zn,

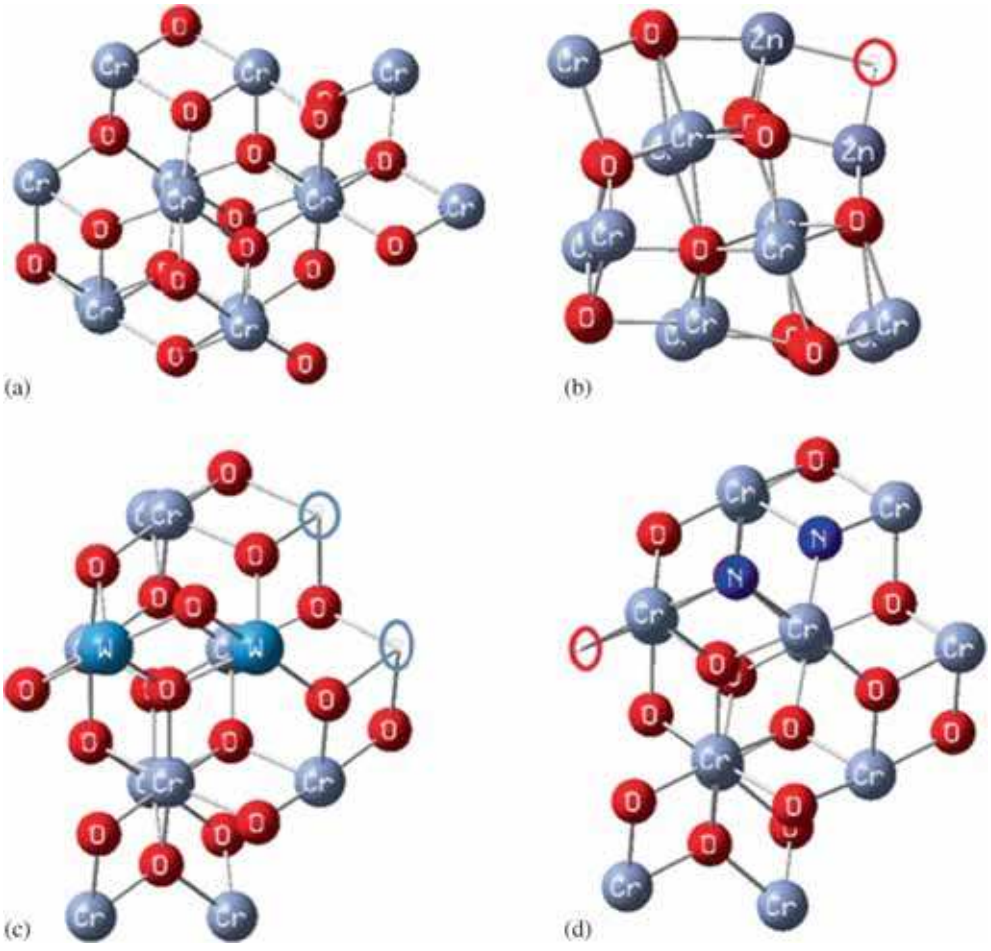

Figure 1. (a) Pristine α-Cr_2O_3 nanostructure; (b) Zn-substituted α-Cr_2O_3 nanostructure; (c) W-substituted α-Cr_2O_3 nanostructure; (d) N-substituted α-Cr_2O_3 nanostructure.

W and N in α-Cr_2O_3 nanostructures. The substitution of impurities on α-Cr_2O_3 nanostructure influences the conductivity enormously. This infers that the adsorption properties of Cl_2 on α-Cr_2O_3 nanostructures can be improved with the incorporation of dopant. Figure 1 (a) – (d) represents the nanostructures of pristine, Zn, W and N-substituted α-Cr_2O_3 nanostructures, respectively. The structure of α-Cr_2O_3 is built from International Centre for Diffraction Data (ICDD) card number: 06-0504. The pristine α-Cr_2O_3 nanostructure has seventeen oxygen atoms and thirteen chromium atoms. Zn-substituted α-Cr_2O_3 nanostructure contains sixteen O atoms, eleven Cr atoms and two Cr atoms are replaced with equivalent two Zn atoms. Similarly, W-substituted α-Cr_2O_3 nanostructure has seventeen O atoms, nine Cr atoms and two Cr atoms are replaced with two W atoms. N-substituted α-Cr_2O_3 nanostructure contains fourteen O atoms, thirteen Cr atoms and two O atoms are replaced with two N atoms. Moreover, Dutta *et al*. have reported CO adsorption on ionic Pt, Pd and Cu sites in $Ce_{0.98}M_{0.02}O_{2-\delta}$.[19] In order to balance the charge in the nanostructure, positive or negative ions should be removed. In a similar way, to maintain charge balance in impurity substituted α-Cr_2O_3 nanostructures, some of the positive or negative ions are removed. Besides, to make charge balance in Zn-substituted α-Cr_2O_3 nanostructure, one oxygen vacancy has been created. Since, the oxidation state of Cr is +3 state and Zn is +2 state. Thus, for substitution of every two Zn atom in α-Cr_2O_3 nanostructure, one oxygen vacancy must be created. Similarly, in the case of W-substituted α-Cr_2O_3 nanostructures, two Cr atoms are removed and for N-substituted α-Cr_2O_3 nanostructures, one oxygen vacancy is created to maintain charge balance in α-Cr_2O_3 base material.

The reason behind the selection of Zn atom is Cr and Zn belongs to fourth period transition metals. Moreover, W is substituted in place of Cr, since Cr and W belongs to group VIB elements. N atom has one electron deficient than O atom, which will increase the p-type behaviour in the base material. The substitution of Zn, W and N completely modifies the conducting properties of α-Cr_2O_3 nanostructures.

3.1 *Structural stability and electronic properties of α-Cr_2O_3 nanostructures*

The structural stability of pristine, Zn, W and N-substituted α-Cr_2O_3 nanostructures are described with formation energy as shown in equation 1,

$$E_{form} = E(\alpha - Cr_2O_3 \text{nanostructure}) - x\,E(Cr) - y\,E(O) - z\,E(\text{dopant}) \quad (1)$$

where E (α-Cr_2O_3 nanostructure) refers the total energy of α-Cr_2O_3 nanostructures, E(Cr), E(O) and E(dopant) represents the corresponding energy of isolated Cr, O and dopant atoms namely Zn, W and N. Meanwhile, x, y and z represents the number of Cr, O and dopant atoms, respectively. The dipole moment, point group and formation energies of pristine, Zn, W and N-substituted α-Cr_2O_3 nanostructures are tabulated in table 1. The formation energy of pristine, Zn, W and N-substituted α-Cr_2O_3 nanostructures are −162.93, −146.88, −144.16 and −161.84 eV, respectively. Before investigating the adsorption characteristics, the stability of the α-Cr_2O_3 material must be studied. The stability of α-Cr_2O_3 base material decreases with the substitution of Zn, W and N atoms as dopants which arise due to decrease in formation energy. However, the electronic properties of α-Cr_2O_3 nanostructures are influenced with substitution impurities. The dipole moment (DP) gives significance about the distribution of charges in α-Cr_2O_3 nanostructure. The DP values for pristine, Zn, W and N-substituted α-Cr_2O_3 nanostructure are found to be 8.45, 10.94, 30.41 and 7.49 Debye, respectively. Moreover, the uniform charge distribution is noticed in pristine, Zn and N-substituted α-Cr_2O_3 nanostructure due to low value of DP. Furthermore, a uniform charge distribution in α-Cr_2O_3 nanostructure can be achieved with the substitution of N in the proper site. In contrast, the substitution of W in α-Cr_2O_3 results in high value of DP. Besides, C_1 point group is observed for all α-Cr_2O_3 nanostructures, which exhibit only identity operation.

The electronic properties of pristine, Zn, W and N-substituted α-Cr_2O_3 nanostructures are illustrated in terms of highest occupied molecular orbital (HOMO) and lowest unoccupied molecular orbital (LUMO).[20] The HOMO-LUMO gap for pristine, Zn, W and N-substituted α-Cr_2O_3 nanostructures are 3.72, 4.02, 3.09 and 3.74 eV, respectively. The experimental energy gap value is reported as 3.4 eV, which almost matches with the obtained theoretical value of 3.72 eV for pristine α-Cr_2O_3. Moreover, the energy gap variation differs with respect to the choice of basis set. Theoretically, DFT method is more probably related to ground state, the excited electronic state may be underestimated. However, the HOMO-LUMO gaps of Cl_2 adsorbed on α-Cr_2O_3 nanostructures are relatively compared with its isolated counterpart. The HOMO-LUMO gap of α-Cr_2O_3 nanostructures increases for Zn and N substitution and in contrast, HOMO-LUMO gap decreases for W substitution. These variations in HOMO-LUMO gap arises due to orbital overlapping of Zn, W and N with Cr and O atoms in α-Cr_2O_3 nanostructure. The HOMO, LUMO level and energy gap of α-Cr_2O_3 nanostructures

Table 1. Calculated energy, dipole moment and point group of α-Cr_2O_3 nanostructures.

Nanostructures	Formation energy (eV)	Dipole moment (Debye)	Point Group
pristine α-Cr_2O_3nanostructure	−162.928	8.45	C_1
Zn-substituted α-Cr_2O_3 nanostructure	−146.88	10.94	C_1
W-substituted α-Cr_2O_3 nanostructure	−144.16	30.41	C_1
N-substituted α-Cr_2O_3 nanostructure	−161.84	7.49	C_1

Table 2. HOMO – LUMO gap of α-Cr_2O_3 nanostructures.

Nanostructures	HOMO (eV)	LUMO (eV)	E_g (eV)
pristine α-Cr_2O_3 nanostructure	−5.64	−1.92	3.72
Zn-substituted α-Cr_2O_3 nanostructure	−5.37	−1.35	4.02
W-substituted α-Cr_2O_3 nanostructure	−6.3	−3.21	3.09
N-substituted α-Cr_2O_3 nanostructure	−5.03	−1.29	3.74

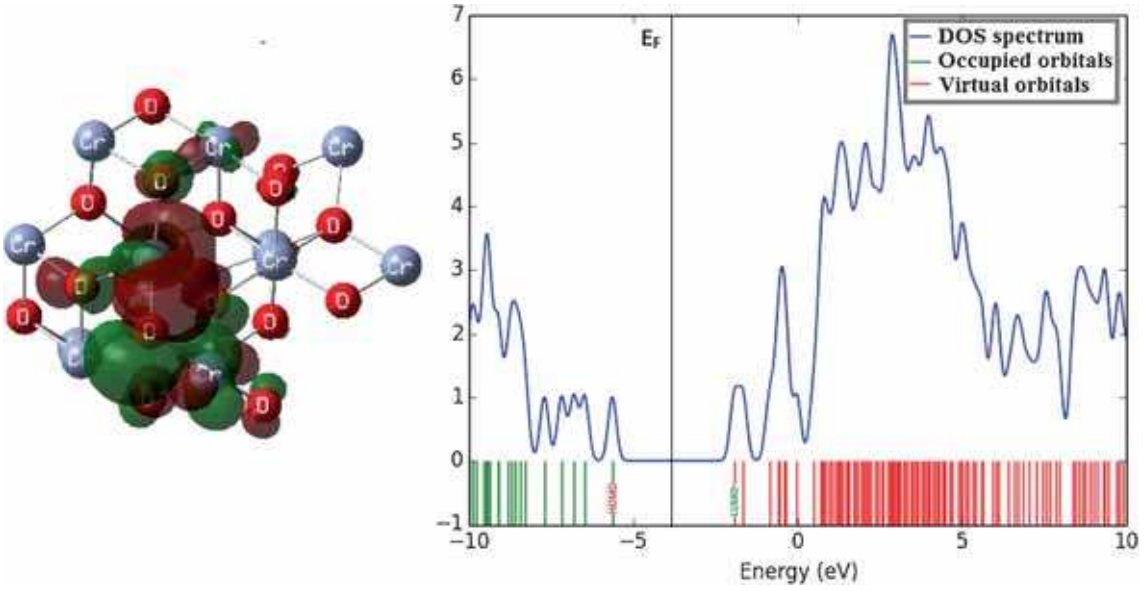

Figure 2. HOMO-LUMO gap and density of states of pristine α-Cr_2O_3 nanostructures.

are tabulated in table 2. With the help of density of states (DOS) spectrum, localization of charges in various energy intervals for α-Cr_2O_3 nanostructures can be illustrated. The DOS spectrum and visualization of HOMO-LUMO gap of α-Cr_2O_3 nanostructure are shown in figure 2. The HOMO-LUMO visualization and density of states of Zn-substituted α-Cr_2O_3, W-substituted α-Cr_2O_3 and N-substituted α-Cr_2O_3 nanostructures are shown in supplementary information figure S2 a-c, respectively. In the present work, for all α-Cr_2O_3 nanostructures, localization of charges are recorded to be more in virtual orbital, which is observed with more peak maxima. These peak maxima in α-Cr_2O_3 nanostructures arise due to the orbital overlapping of Cr atoms with O atoms in α-Cr_2O_3 base material. Besides, the peak maxima in virtual orbitals of α-Cr_2O_3 base material are more feasible for adsorption of gas molecules, since the transition of electrons takes place easily between virtual orbital of α-Cr_2O_3 and target gas molecules.

The electronic properties of α-Cr_2O_3 nanostructure can also be illustrated with the help of ionization potential (IP) and electron affinity (EA).[21,22] Figure 3 represents IP and EA of α-Cr_2O_3 nanostructures. Generally IP depicts the quantity of energy required to remove electron from α-Cr_2O_3 nanostructures and the EA depicts the energy variation owing to addition of electron in α-Cr_2O_3 nanostructures. The high value of IP implies that the electrons are perfectly bounded to nucleus in α-Cr_2O_3 nanostructure. Different trends are observed on both ionization potential and electron affinity of α-Cr_2O_3 nanostructure. Relatively, less energy is

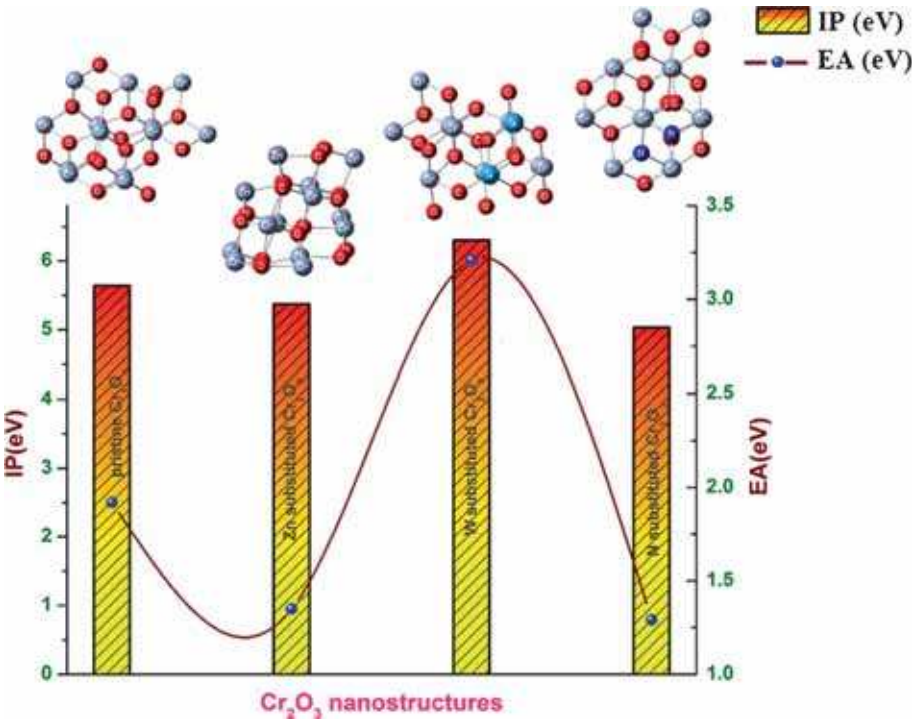

Figure 3. IP and EA of α-Cr_2O_3 nanostructure.

required to remove electrons from α-Cr_2O_3 nanostructure due to the substitution of Zn and N atoms. However, W substitution on α-Cr_2O_3 nanostructure gives rise to high value of IP. EA is one of the important criterions in plasma physics and chemical sensors. The EA values of pristine, Zn, W and N-substituted α-Cr_2O_3 nanostructures are 1.92, 1.35, 3.21 and 1.29 eV, respectively.

3.2 *Adsorption characteristics of Cl_2 on α-Cr_2O_3 nanostructures*

In the beginning of Cl_2 adsorption study on α-Cr_2O_3, Cl_2 molecule should be investigated in gas phase. The bond length between two chlorine atoms is 1.98 Å and the bond length between chromium and oxygen atom in α-Cr_2O_3 is 1.82 Å. During the optimization of α-Cr_2O_3 nanostructure, these bond lengths are utilized. Figure 4(a) refers the adsorption of Cl atom in Cl_2 molecules adsorbed on Cr atom in pristine α-Cr_2O_3 nanostructure and it is denoted by position A. Figure 4 (b) depicts the adsorption of Cl atom in Cl_2 gas molecule adsorbed on O atom of pristine α-Cr_2O_3 nanostructure and it is mentioned as position B. The other positions are represented as figure S4 (c) in Supplementary Information.

The adsorbed energy of Cl_2 gas molecule on α-Cr_2O_3 nanostructure can be expressed by equation (2) as

$$E_{ad} = [E(Cr_2O_3/Cl_2) - E(Cr_2O_3) - E(Cl_2)] \quad (2)$$

where $E(Cr_2O_3 / Cl_2)$ denotes the energy of Cr_2O_3/Cl_2 complex, $E(Cr_2O_3)$ and $E(Cl_2)$ are the isolated energies of Cr_2O_3 and Cl_2 molecules, respectively. When Cl_2 molecules are adsorbed on α-Cr_2O_3 material, the positive and negative values of adsorbed energy (E_{ad}) are represented as endothermic and exothermic specificity, respectively. In the present work, positions A, C and H have exothermic specificity. This infers that the energies are transferred from α-Cr_2O_3 material to Cl_2 molecules, which are specified by negative value of adsorbed energy. In contrast, for remaining positions B, D, E, F, G, I, J and K belong to endothermic specificity. This depicts that the energies are transferred from Cl_2 molecule to α-Cr_2O_3 material, which is referred as positive value of adsorbed energy. The E_{ad} values of α-Cr_2O_3 base material for positions A – K are −0.54, 0.27, −0.54, 2.18, 0.001, 2.72, 1.90, −0.27, 0.27, 0.82 and 2.45 eV, respectively. Furthermore, the conductivity of α-Cr_2O_3 nanostructure decreases owing to widening of band gap when Cl_2 gets adsorbed on α-Cr_2O_3 nanostructure, which can be compared with its isolated counterpart. When Cl_2 gets adsorbed on positions A to K of α-Cr_2O_3 nanostructure, the corresponding HOMO-LUMO gap values are 4.28, 4.39, 4.01, 4.04, 4.91, 4.16, 3.01, 3.25, 3.84, 4.86 and 4.79 eV. From the observation, it is inferred that the adsorbed energy and HOMO-LUMO gap of α-Cr_2O_3 nanostructure varies when Cl_2 gets adsorbed on α-Cr_2O_3 nanostructure, which indicates

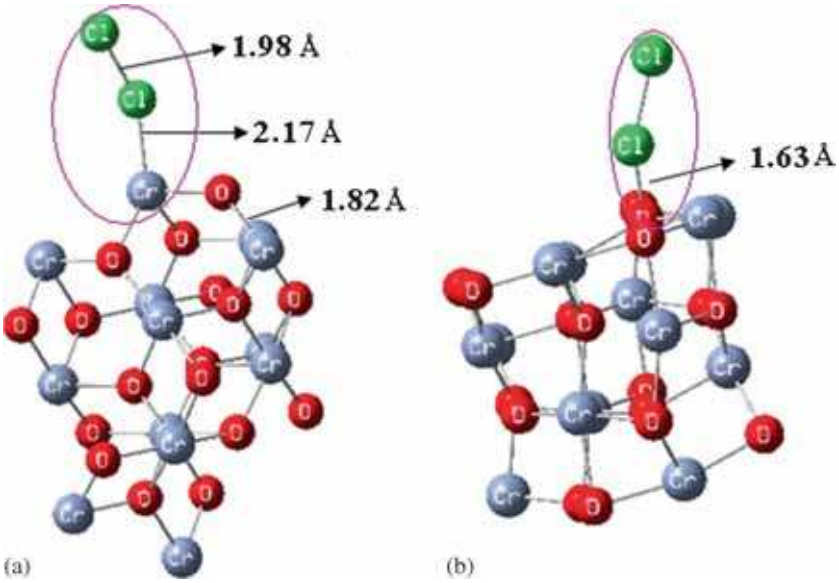

Figure 4. (a) Cl_2 adsorbed on position 'A'; (b) Cl_2 adsorbed on position 'B'.

that α-Cr_2O_3 nanostructure can be efficiently used to sense Cl_2 gas molecule.

Han *et al.*[23] reported sodium super ionic conductor (NASICON) based potentiometric Cl_2 sensor combining NASICON with Cr_2O_3 sensing electrode. In the reported work, authors highlight the sensing performance of Cl_2 sensor in air based NASICON and oxide electrode. They report that Cr_2O_3 single oxide shows a high sensitivity to chlorine gas in air atmosphere at 300°C. Nigussa *et al.*[24] proposed the adsorption of hydrogen, chlorine, and sulfur on α-Cr_2O_3 (0001) surfaces through density functional theory. Chlorine, hydrogen and sulfur get adsorbed on Cr_2O_3 and Cr terminated α-Cr_2O_3 surfaces in the reported work. It was reported that S and Cl atoms are strongly adsorbed on the surface of Cr in α-Cr_2O_3. The results are in accordance with that of the present work. Balouria *et al.*[25] give a clear picture on the temperature dependent H_2S and Cl_2 sensing characteristics on Cr_2O_3 thin films. Cr_2O_3 thin films are synthesised by electron-beam deposition method and gas sensing properties of Cr_2O_3 are studied for various gases namely CH_4, Cl_2, CO, H_2S and NH_3 at the operating temperature between 30 and 300°C with gas concentration in the range of 1-30 ppm. Nigussa *et al*. reported highly selective Cl_2 sensing characteristics on Cr_2O_3 at the temperature of 220°C. In this work, the transfer of electrons between α-Cr_2O_3 base material and Cl_2 gas molecules leads to change in conductivity. It is observed that the pristine, Zn, W and N substituted Cr_2O_3 nanostructures are the prominent base material for sensing chlorine. The most suitable adsorption site of Cl_2 gas molecule on Cr_2O_3 material can be established only after investigating the percentage of average energy gap variation along with its relative isolated counterpart. Table 3 represents HOMO-LUMO gap, percentage variation in energy gap, adsorbed energy and Mulliken population analysis. From the observation of these results, it is revealed that the most prominent adsorption site of Cl_2 gas molecules on Cr_2O_3 nanostructure are positions E, F, J and K. The adsorption of Cl atom in Cl_2 molecules adsorbed on Zn and Cr in Zn and W-substituted Cr_2O_3 nanostructure, respectively. The average energy gap variation is given by equation (3) as

$$E_g^a\,(\%) = \frac{Eg(Cr203/Cl2) - Eg(Cr203)}{Eg(Cr203/Cl2)} \times 100 \quad (3)$$

where $E_g(Cr_2O_3/Cl_2)$ is the energy gap of the base material with adsorbed Cl_2 and $E_g(Cr_2O_3)$ is the energy gap of isolated α-Cr_2O_3 base material. Furthermore, the adsorption of Cl atom in Cl_2 molecules adsorbed on both O and N in N-substituted Cr_2O_3 nanostructure is found to be the most favourable site. Since, the average energy gap variations are recorded high when compared to other adsorption sites.

The transfer of electrons between Cl_2 molecule and α-Cr_2O_3 material can be analysed by Mulliken population analysis (Q).[26–35] The negative charge of Mulliken population refers that the electrons are transferred from α-Cr_2O_3 material to Cl_2 gas molecules and in contrast, the positive charge of Q depicts the electrons transferred from Cl_2 gas molecules to α-Cr_2O_3 material. The Mulliken population values of pristine α-Cr_2O_3 nanostructure for positions A and B are found to be 0.002 and −0.25 **e**, respectively. In the case of impurity

Table 3. Adsorbed energy, Mulliken population, HOMO-LUMO gap and average energy gap variation of α-Cr_2O_3 nanostructures.

Nanostructures	E_{ad} (eV)	Q (e)	E_{HOMO}	E_{FL} (eV)	E_{LUMO}	E_g (eV)	E_g^a %
pristine α-C_2O_3 nanostructure	–	–	−5.64	−3.78	−1.92	3.72	–
A	−0.544	0.002	−6.31	−4.17	−2.03	4.28	13.08
B	0.272	−0.254	−6.85	−4.65	−2.46	4.39	15.26
Zn-substituted α-C_2O_3 nanostructure	–	–	−5.37	−3.36	−1.35	4.02	–
C	−0.544	0.024	−5.37	−3.36	−1.36	4.01	0.25
D	2.176	−0.242	−5.84	−3.82	−1.8	4.04	0.5
E	0.001	0.039	−6.42	−3.96	−1.51	4.91	18.13
W-substituted α-C_2O_3 nanostructure	–	–	−6.3	−4.755	−3.21	3.09	–
F	2.72	0.085	−6.48	−4.4	−2.32	4.16	25.72
G	1.904	0.42	−5.98	−4.47	−2.97	3.01	2.66
H	−0.272	−0.218	−6.26	−4.63	−3.01	3.25	4.92
N-substituted α-C_2O_3 nanostructure	–	–	−5.03	−3.16	−1.29	3.74	–
I	0.272	0.043	−5.15	−3.23	−1.31	3.84	2.6
J	0.816	−0.224	−6.87	−4.44	−2.01	4.86	23.05
K	2.448	0.114	−6.36	−3.96	−1.57	4.79	21.92

substituted α-Cr_2O_3 nanostructures for the positions C, D, E, F, G, H, I, J and K have Q values of 0.024, −0.242, 0.039, 0.085, 0.42, −0.218, 0.043, −0.224 and 0.114 e, respectively. From the observation, positions A, C, E, F, G, I and K have positive value of Q, which implies that the electrons are transferred from Cl_2 to α-Cr_2O_3 base material and for the remaining positions B, D, H and J have negative values of Q, which infers that the electrons are transferred from α-Cr_2O_3 base material to Cl_2. Almost same negative value of Mulliken charge are recorded for positions B, D, H and J, but the corresponding adsorbed energy values differ. Moreover, with the substitution of W and N on α-Cr_2O_3 material, E_{ad} increases and the corresponding average energy gap variation (E_g^a) also increases drastically. This may be due to increase in hole concentration in α-Cr_2O_3 base material with the substitution of W and N. The substitution of N atoms leads to deficiency of electrons, which in turn increases the p-type behaviour. From the observation it is inferred that Zn, W and N-substituted α-Cr_2O_3 nanostructures are promising material for Cl_2 sensing. Analysing all the parameters such as adsorbed energy, Mulliken population and average energy gap variation for impurity substituted α-Cr_2O_3 nanostructures are found to be more probable. The adsorbed energy, average energy gap variation and energy gap for Zn-substituted α-Cr_2O_3 nanostructure is significant, even if Mulliken charge transfer is low. Likewise, W and N-substituted α-Cr_2O_3 nanostructure also shows favourable adsorption characteristics of Cl_2 on α-Cr_2O_3

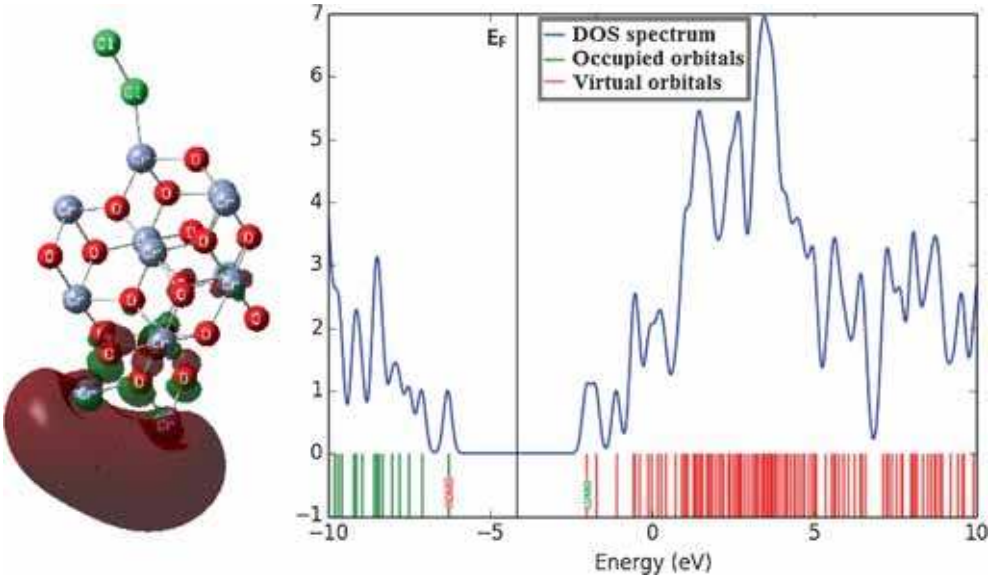

Figure 5. HOMO-LUMO visualization and density of states of Cl_2 adsorbed on position A of α-Cr_2O_3 nanostructures.

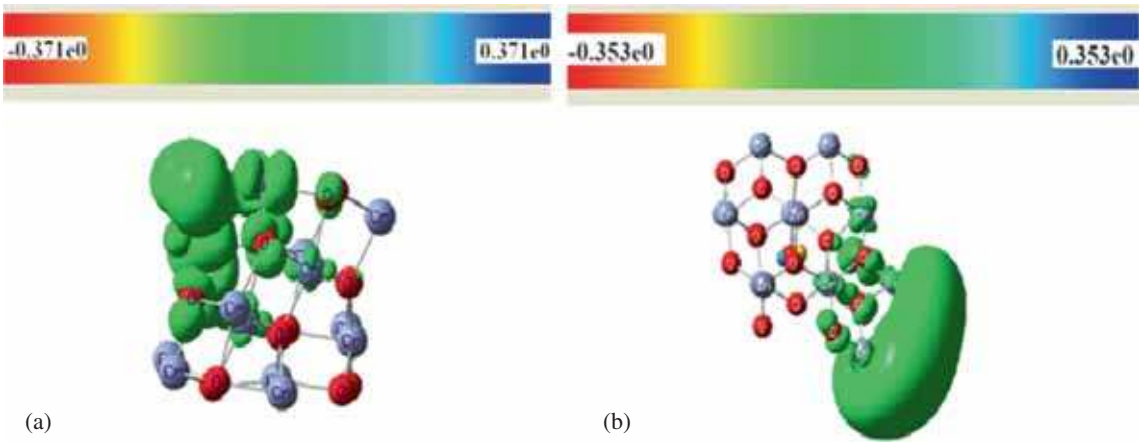

Figure 6. (a) Electron density of pristine α-Cr_2O_3 nanostructure; (b) Electron density of Zn-substituted α-Cr_2O_3 nanostructure.

nanostructure. The average energy gap variation, adsorbed energy and energy gap is found to be noteworthy. However, in the case of W-substituted α-Cr_2O_3 nanostructure, the adsorption properties of Cl_2 are not favourable, when Cl atom in Cl_2 molecules adsorbed on O and W atoms in W-substituted α-Cr_2O_3 nanostructure. Even though the adsorbed energy is more, the average energy gap variation and energy gap is not feasible for Cl_2 adsorption. Therefore, the most favourable adsorption sites can be found only after investigation of adsorbed energy, Mulliken population and HOMO – LUMO gap of α-Cr_2O_3 nanostructure. Figure 5a represents density of states (DOS) spectrum and HOMO – LUMO gap of Cl_2 adsorbed on α-Cr_2O_3 material for position A. The HOMO-LUMO visualization and density of states of Cl_2 adsorbed on positions B to K of α-Cr_2O_3 nanostructures are illustrated in supplementary information figure S5, (c)-(k). From the density of states spectrum, it is clearly inferred that the more peak maxima are observed in the virtual orbital rather than the occupied orbital. This implies that the electrons can easily transfer between Cl_2 molecule and α-Cr_2O_3 material, which can be used as an efficient chemical sensor. Figure 6 (a) and (b) represent the electron density of pristine α-Cr_2O_3 and Zn-substituted α-Cr_2O_3 nanostructures, respectively. The electron density of W-substituted α-Cr_2O_3 nanostructure and N-substituted α-Cr_2O_3 nanostructures are shown in supplementary information as figure S6, (c) and (d). Figure 7 depicts the electron density for various positions A and B and the electron density of remaining positions C to K are shown in figure S7 (c)-(k) in the Supplementary Information. The electron density can be precisely observed with the magnitude of colour gradient. Among all the positions, E, F, J and K are the most prominent site for Cl_2 adsorption on α-Cr_2O_3. Since, the corresponding

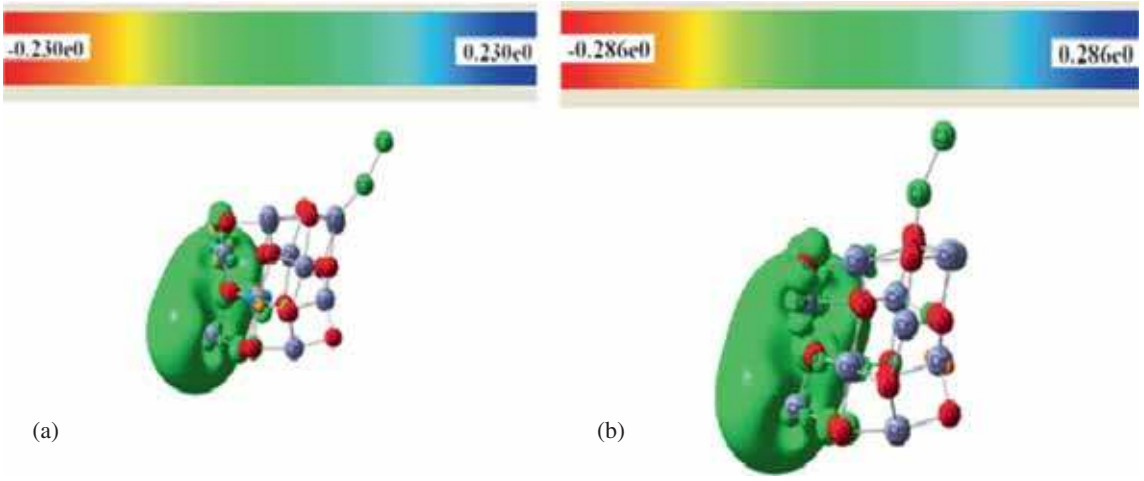

Figure 7. (a) Electron density on position 'A'; (b) Electron density on position 'B'.

Table 4. Selectivity of Cl_2 gas in mixed atmosphere.

Nanostructures	E_{ad} (eV)	Q (e)	E_{HOMO}	E_{FL} (eV)	E_{LUMO}	E_g (eV)	E_g^a %
pristine Cr_2O_3	–	–	−5.64	−3.78	−1.92	3.72	–
pristine Cr_2O_3-Cl_2	−0.544	0.002	−6.31	−4.17	−2.03	4.28	13.08
pristine Cr_2O_3-CO	−2.448	0.147	−6.57	−4.51	−2.45	4.12	9.71
pristine Cr_2O_3-H_2S	−3.561	0.251	−6.49	−4.55	−2.61	3.88	4.12
pristine Cr_2O_3-NO	−3.601	0.263	−6.65	−4.68	−2.71	3.94	5.58

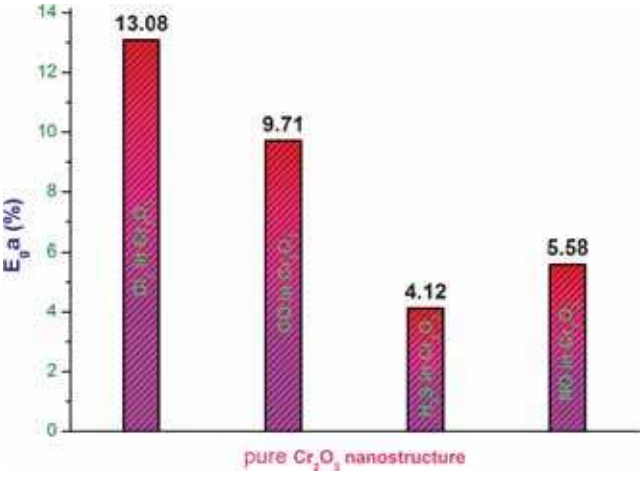

Figure 8. Selectivity of Cl_2 in mixed atmosphere.

magnitude value of electron density is high, which is optimum for catalytic behaviour. From all the observations, Cl_2 sensing properties can be enhanced with Zn, W and N substitution in α-Cr_2O_3 base material.

3.3 *Selectivity of α-Cr_2O_3 nanostructures*

Selectivity, sensitivity and stability (SSS) are the significant parameters for detection of target gas by the metal oxide nanostructures. Table 4 refers the selectivity of Cl_2 gas in the mixed atmosphere. Figure 8 shows precise comparison between Cl_2 gas and other gases found in the atmosphere such as CO, H_2S and NO when get adsorbed on to α-Cr_2O_3 base material. As we discussed above the important parameters such as Mulliken charge, energy gap, adsorption energy and average energy gap variation are taken into consideration for finding the selectivity of Cl_2 gas in mixed environment. As a result, α-Cr_2O_3 nanostructure is selective towards Cl_2 gas among other gases namely CO, H_2S and NO. Moreover, the average energy gap variation of Cl_2 adsorbed in α-Cr_2O_3 material is more when compared to CO, H_2S and NO adsorbed in α-Cr_2O_3 material. Thus, it can be concluded that α-Cr_2O_3 nanostructures is a promising material, which can be used as a sensing material for Cl_2 gas in mixed gas environment.

4. Conclusions

In conclusion, the DFT method is utilized to study the chlorine adsorption characteristics on α-Cr_2O_3 material along with B3LYP/ LanL2DZ basis set. The electronic properties and structural stability of pristine, Zn, W and N-substituted α-Cr_2O_3 nanostructures are investigated. The electronic properties of α-Cr_2O_3 nanostructures are studied by HOMO-LUMO gap, electron affinity and ionization potential. The structural stability of α-Cr_2O_3 nanostructures are illustrated in terms of formation energy. The most prominent adsorption sites of Cl_2 on α-Cr_2O_3 nanostructures are identified with adsorbed energy, average energy gap variation, Mulliken population analysis and HOMO-LUMO gap. The adsorption characteristics of chlorine on α-Cr_2O_3 material can be improved with substitution of Zn, W and N as dopant element in α-Cr_2O_3. Thus, the most suitable adsorption site of Cl_2 on α-Cr_2O_3 nanostructures is when the Cl atom in Cl_2 is adsorbed on Zn and Cr in Zn and W-substituted Cr_2O_3 nanostructure, respectively, followed by the Cl atom in Cl_2 adsorbed on both O and N in N-substituted Cr_2O_3. α-Cr_2O_3 nanostructure is a promising material for sensing Cl_2 gas in a mixed gas environment.

Supplementary Information

Figures S1 to S7 are available at www.ias.ac.in/chemsci.

References

1. Korotcenkov G, Han S H and Cho B K 2013 *J. Sensor Sci. Technol.* **22** 1
2. Chen P C, Shen G and Zhou C 2008 *IEEE Trans. Nanotechnol.* **7** 668
3. Arnold C, Harms M and Goschnick J 2002 *IEEE Sens. J.* **2** 179
4. Aswal D K and Gupta S K 2007 In *Science and Technology of Chemiresistive Gas Sensors* 2nd Ed. (Nova Science Publisher: New York)
5. Moseley P T 1997 *Meas. Sci. Technol.* **8** 223
6. Cantalini C 2004 *J. Eur. Ceram. Soc.* **24** 1421
7. Cellard A V, Garnier G, Fantozzi G, Baret and Fort P 2009 *Ceram. Int.* **35** 913

8. El-Molla S A 2005 *Appl. Catal., A* **280** 189
9. Morrison S 1977 *J. Catal.* **47** 69
10. Saroha A K 2006 *JCHAS* **13** 5
11. Frank M, Rivera R and Stashans A 2012 *Physica B* **407** 1262
12. Blacklocks A N, Atkinson A, Packer R J, Savin S L P and Chadwick A V 2006 *Solid State Ionics* **177** 2939
13. Dinadayalane T C, Paytakov G and Leszczynski J 2013 *J. Mol. Model.* **19** 2855
14. Frisch M J, Trucks G W, Schlegel H B, Scuseria G E, Robb M A, Cheeseman J R, Scalmani G, Barone V, Mennucci B, Petersson G A, Nakatsuji H, Caricato M, Li X, Hratchian H P, Izmaylov A F, Bloino J, Zheng G, Sonnenberg J L, Hada M, Ehara, Toyota K, Fukuda R, Hasegawa J, Ishida M, Nakajima T, Honda Y, Kitao O, Nakai H, Vreven T, Montgomery J A, Jr., Peralta J E, Ogliaro F, Bearpark, Heyd J J, Brothers E, Kudin K N, Staroverov V N, Kobayashi R, Normand J, Raghavachari K, Rendell A, Burant J C, Iyengar S S, Tomasi J, Cossi M, Rega N, Millam J M, Klene M, Knox J E, Cross J B, Bakken V, Adamo C, Jaramillo J, Gomperts R, Stratmann R E, Yazyev O, Austin A J, Cammi R, Pomelli C, Ochterski J W, Martin R L, Morokuma K, Zakrzewski V G, Voth G A, Salvador P, Dannenberg J J, Dapprich S, Daniels A D, Farkas Ö, Foresman J B, Ortiz J V, Cioslowski J, and Fox D J 2009 (Gaussian, Inc.: Wallingford CT)
15. Paul K W, Kubicki J D and Sparks D L 2007 *Eur. J. Soil Sci.* **58** 978
16. Becke A D 1988 *Phys. Rev. A: At. Mol. Opt. Phys.* **38** 3098
17. Becke A D 1993 *J. Chem. Phys.* **98** 1372
18. Boyle N M O, Tenderholt A L and Langner K M 2007 *J. Comp. Chem.* **29** 839
19. Dutta G, Gupta A, Waghmare U V and Hegde M S 2011 *J. Chem. Sci.* **123** 509
20. Sriram S and Chandiramouli R 2013 *EPJ Plus* **128** 116
21. Nagarajan V and Chandiramouli R 2014 *Alexandria Engineering Journal* **53** 437
22. Chandiramouli R and Sriram S 2014 *Mater. Sci. Semicond. Process.* **27** 800
23. Zhang Han, Li J, Zhang H, Liang X, Yin C, Diao Q, Zheng J and Lu G 2013 *Sens. Actuators B* **180** 66
24. Nigussa K N, Nielsen K L, Borck Ø and Støvneng J A 2011 *Corros. Sci.* **53** 3612
25. Balouria V, Kumar A, Singh A, Samanta S, Debnath A K, Mahajan A, Bedi R K, Aswal D K, Gupta S K and Yakhmi J V 2011 *Sens. Actuators B* **157** 466
26. Mulliken R S 1955 *J. Chem. Phys.* **23** 1833
27. Csizmadia I G 1976 In *Theory and Practice of MO Calculations on Organic Molecules* (Elsevier: Amsterdam, Oxford, New York) p. 159
28. Nagarajan V and Chandiramouli R 2014 *Ceram. Int.* **40** 16147
29. Nagarajan V and Chandiramouli R 2014 *Comp. Theor. Chem.* **1049** 20
30. Nagarajan V and Chandiramouli R 2014 *Struct. Chem.* **25** 1765
31. Beheshtian J, Zargham B, Mohammad K and Ahmadi A 2011 *J. Mol. Model.* **18** 2653
32. Beheshtian J, Peyghan A A and Zargham B 2012 *Physica E* **44** 1963
33. Nagarajan V and Chandiramouli R 2014 *J. Inorg. Organomet. Polym.* **24** 1038
34. Nagarajan V and Chandiramouli R 2015 *J. Inorg. Organomet. Polym.* **25** 837
35. Nagarajan V and Chandiramouli R 2015 *Superlattices Microstruct.* **78** 22